BIOINFORMATION
Discovery at the interface of physical and biological sciences

open access www.bioinformation.net Hypothesis

Volume 9(1)

Evolutionary and functional analysis of fructose bisphosphate aldolase of plant parasitic nematodes

CVS Siva Prasad*, Saurabh Gupta, Himansu Kumar & Murlidhar Tiwari

Division of Applied Sciences & IRCB, Indian Institute of Information Technology, Deoghat, Jhalwa, Allahabad 211012, India; CVS Siva Prasad – Email: shiva@iiita.ac.in; Phone: +91532 2922201; Fax: +91532 2430006; *Corresponding author

Received November 12, 2012; Accepted November 14, 2012; Published January 09, 2013

Abstract:
The essential and ubiquitous enzyme fructose bisphosphate aldolase (FBPA) has been a good target for controlling the various types of infections caused by pathogens and parasites. The parasitic infections of nematodes are the major concern of scientific community, leading to biochemical characterization of this enzyme. In this work we have developed a small dataset of all types of FBPA sequences collected from publically available databases (EMBL, NCBI and Uni-Port). The Phylogenetic study shows that evolutionary relationships among sequences of FBPA are clustered into three main groups. FBPA sequences of *Globodera rostochiensis* (FBPA_GR) and *Heterodera glycines* (FBPA_HG) are placed in group II, sharing the similar evolutionary relationship. The catalytic mechanism of these enzymes depends upon which class of aldolase, it belongs. The class of enzyme has been confirmed on the basis of sequences and structural similarity with template structure of class I FBPA. To confirm catalytic mechanism of above said model structures, the known substrate fructose-1, 6-bisphosphate (FBP) and competitive inhibitor Mannitol-1, 6 bisphosphate (MBP) were docked at known catalytic site of enzyme of interest. The comparative docking analysis shows that enzyme-substrate complex is forming similar Schiff base intermediate and conducts C_3–C_4 bond cleavage by forming Hydrogen bonding with reaction catalyzing Glu-191, reactive Lys-150, and Schiff base forming Lys-233. On the other hand enzyme-inhibitor noncovalent complex is forming cabinolamine precursor and the proton transfer by the formation of hydrogen bond between MBP O_2 with Glu191 enabling stabilization of cabinolamine transition state, which confirms the similar inhibition mechanism. Thus we conclude that Plant Parasitic Nematodes (PPNs) have evolutionary and functional relationship with the class I aldolase enzyme. Hence, FBPA can be targeted to control plant parasitic nematodes.

Keywords: FBPA, FBPA_HG, 1ZAH_A, FBP, MBP, PPNs, Modeling, Simulation & Docking.

Background:
The parasitic nematodes are commonly found in humans, rats, pigs, plants and other species. Various types of PPNs are causing infections to worldwide consumed crops like *Glycine max*, *Triticum spp.*, *Oryza spp.* and *Solanaceae spp* **[1].** The vital life processes of PPNs mainly depend upon carbohydrate metabolism. The probe of the glycolytic pathway offers insight into development of controlling strategies based on energy production **[2].** FBPA is a key enzyme of Glycolytic pathway and responsible for the reversible cleavage of fructose 1, 6-bisphosphate (FBP) to glyceraldehyde 3-phosphate (G3P) and dihydroxyacetone phosphate (DHAP) **[3].** This enzyme also catalyzes the segmentation of structurally related sugar phosphates including fructose 1-phosphate (Fru 1-P) an intermediate of fructose metabolism. FBPA has standard classification number EC 4.1.2.13 and classified into two classes: Class-I and Class-II. With little exception in both class, aldolase are characterized more in vertebrates and lesser in invertebrates **[4, 5].** Tissue specific class I aldolase are found in animals, plants, green algae and other higher organism **[6].** Three unique forms of class I aldolase have been determined in various tissues of vertebral species, including human. These are aldolase A (found in skeletal muscle and red blood cells), aldolase B (found in small intestine, liver and kidney), and

 © 2013 Biomedical Informatics

aldolase C (found in smooth muscle and neuronal tissues) **[7].** These forms are differentiable on the basis of immunological and kinetic properties **[8].** The class-II aldolase is commonly present in lower organism e.g. bacteria, yeasts, fungi etc. Class-II is divided into group A and B depending upon insertion or deletion in amino acid sequences. Group A, enzymes play major function in glycolysis and gluconeogenesis, while group B enzymes are more heterogeneous and has diverse metabolic roles and substrate specificities **[9].**

The catalytic mechanism of class I and class II aldolase have been extensively studied and it is different in both classes. The class I enzymes use reactive lysine residue in the active site to stabilize a reaction intermediate via Schiff-base formation **[10, 11].** While the class-II enzymes polarize the substrate carbonyl by using divalent metal ion generally zinc. Although tertiary structures of both classes form the $(\beta/\alpha)_8$ barrel fold, also known as the TIM barrel fold, which shares the same overall fold but do not share any significant sequence homology or common catalytic residues as well as distinct location of their active sites **[12].** In present work, we have found out the evolutionary relationship between all available characterized aldolase sequences from nematodes till date. In addition, belonging class and their catalytic mechanism of PPNs aldolase sequences have been dug out using comparative sequence analysis and structural biology approaches.

Methodology:

Collection of FBPA protein sequences

The EMBL, NCBI and Uni-port protein databases were searched with individual key word like aldolase, Fructose-bisphosphate aldolase and Fructose 1, 6-bisphosphate aldolase of nematodes, browsed protein sequences were screened and downloaded. All incomplete sequences were excluded from dataset. Two or more complete sequences which were having 100% sequence identity as determined by the EMBOSS pair wise alignment tool, were removed from dataset **[13].** For each aldolase sequence the locus number, name of the protein, experimentally determined functions and associated references were collected. In our dataset each sequence was allocated a specific name which has a reference code followed by scientific name of the nematodes.

Sequence and Phylogenetic analysis

Multiple sequence alignment (MSA) of dataset sequences were performed by online ClustalW2 Tool **[14].** For initial pair wise alignment, Gonnet protein weight matrix (GPWM) with gap opening penalty 10 and a gap extension penalty 0.1 have been used. For multiple alignments, gap opening penalty 10, gap extension penalty 0.1, GPWM and 5 tree iteration (by Neighbor-Joining method) have been used**.** To assist comparison between PPNs (*Globodera rostochiensis* (FBPA_GR) and *Heterodera glycines* (FBPA_HG)) and other nematodes sequences were included in the alignment. It helped us to find out the percentage similarity of FBPA sequences of PPNs with other dataset sequences. The alignment file viewed and Phylogenetic tree was generated using percentage sequence identity with neighbour-joining algorithm in the Jalview-multiple sequence editor Tool **[15].**

Tertiary structure prediction

The functions of both class enzymes mainly depends upon formation of the TIM barrel fold and present residues in active site. To find out functions of dataset aldolase protein sequences required to generate suitable molecular model. The dataset protein sequences **Table 1 (see supplementary material)** have been subjected for detecting suitable templates for homology modeling against Protein Database PDB **[16].** The template searching was performed using Domain Enhanced Lookup Time Accelerated-BLAST (DELTA-BLAST) **[17].** The best template for each sequence was selected on the basis of similarity, percentage of identity, expectation value, bit scores and query coverage area. The best template structures for each sequence with their validation statistics depicted in **Table 1**. The Chain A of FBPA from Rabbit Muscle (PDB ID: 1ZAH) was common template for sequences except *Nematocida parisii* sequences **[18].** The 1ZAH structure was generated by X-ray diffraction study with 1.80Å resolution. The R factor of the structure was 0.167 and R-free value was 0.205. We have generated molecular models for plant-parasitic nematodes only as they are our prime concern. The models were generated using Modeller 9v10 **[19]** and validated using online server Structural analysis and verification server (SAVS) **[20-23].** Secondary structural investigation and conformation analysis of modeled structures were performed by ProFunc, an online server of PDBsum **[24].** The comparative sequence and structural analysis of active site and formation of TIM barrel fold for modeled structures with template structure have been analyzed by ClustalW2 tool and USFChimera.

Simulation and validation of models

The sequences and structural comparison between generated models of FBA_HG shows 99.9% sequence similarity with similar active site residues and sharing same homology of 3D Structure. To find out stable active sites and role of TIM barrel fold in catalytic mechanism, we performed simulation of model FBPA_HG structure using GROMACS 4.5.3 package **[25, 26].** To understand mechanism with exact comparison, we also performed molecular dynamics (MD) for template structure 1ZAH_A. Selected both structure were subjected for energy minimization using OPLS-AA/L force field **[27].** In the subsequent steps the structure of FBA_HG and 1ZAH_A were embedded in a cubic box containing SPC216 water molecules **[28].** Normal charge states of ionizable groups at pH 7 for FBPA_HG and 1ZAH_A have been neutralized by adding respective ions in the system. Energy minimization was performed after this ion treatment. The next step of the protocol was to maintain the equilibrium of the system which was performed in two phases. The first phase include the NVT ensemble, a short 100 picoseconds (ps) position-restrained MD simulation at 300K was carried out using a Berendsen thermostat to ensure the proper stabilization of the temperature. The second phase include NPT ensemble for 100ps position-restrained MD simulation at 300K and 1 bar was carried out using a Parrinello-Rahman barostat pressure coupling to stabilize the system with respect to pressure and density **[29].** Finally unrestrained 10 nanoseconds (ns) MD simulation was initiated on the NPT ensemble for both structures. The quality checks on the MD simulations were performed by GROMACS applications. The numerical graphs and interpretation of data were performed using Xmgrace software. The structures which were qualifying the all validation parameters with good scores were further subjected for docking analysis.

© 2013 Biomedical Informatics

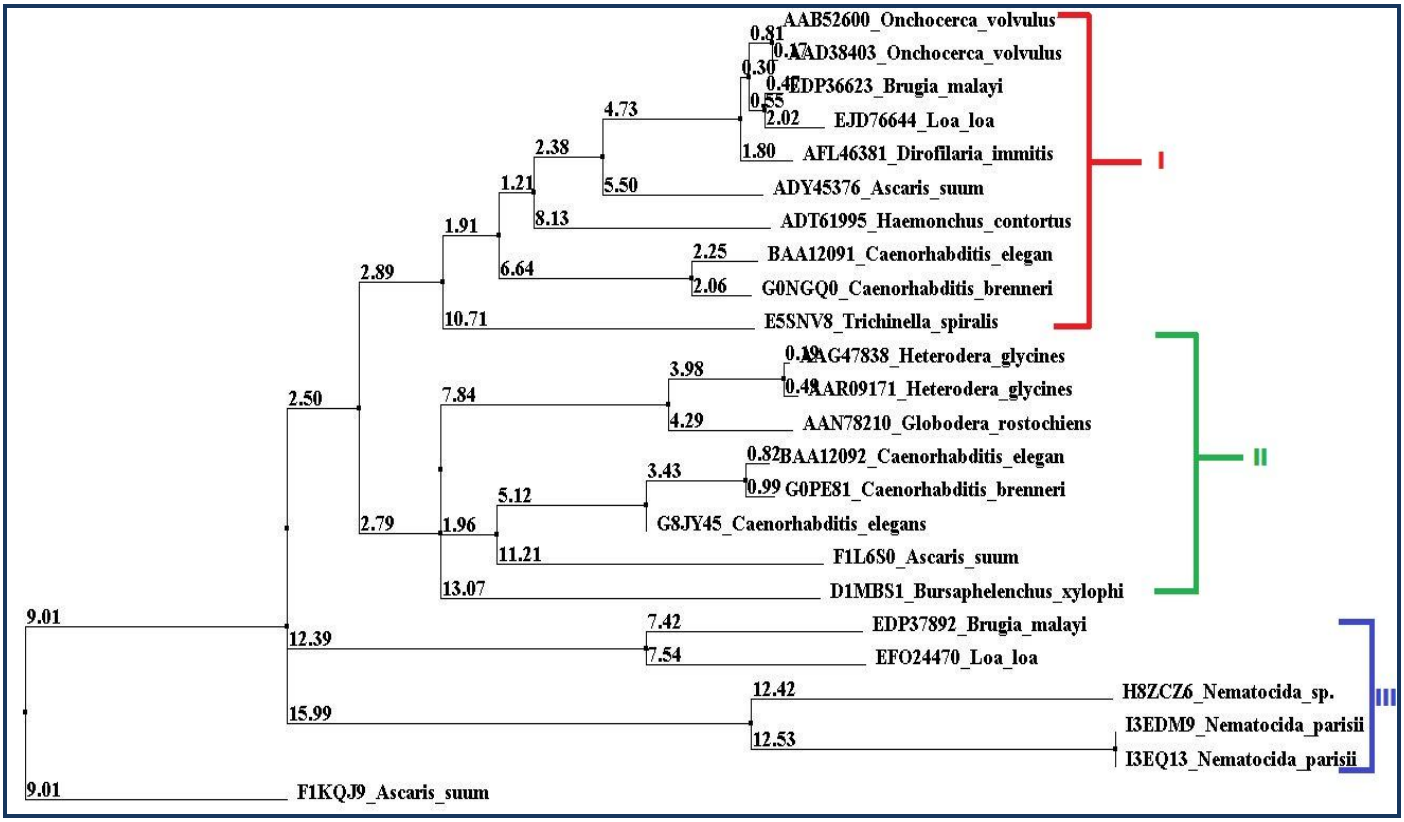

Figure 1: Phylogenetic tree for selected 24 FBPA protein sequences from different nematodes were classified into three major groups (I- Red, II-Green and III-Blue) with their respective distances.

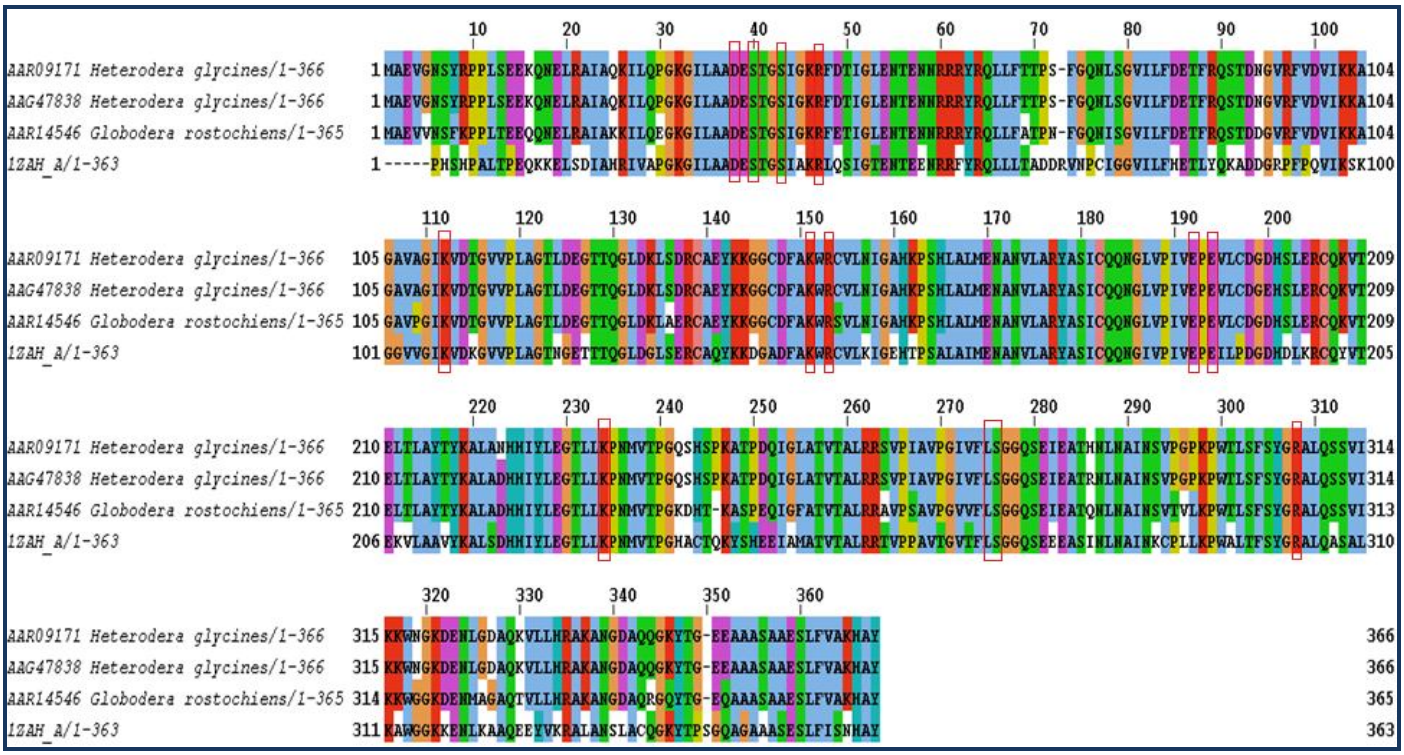

Figure 2: Multiple sequence alignment of FBPA sequences of PPNs with template structure sequence. The common active site amino acid residues are marked with rectangular red boxes.

Docking of substrate and competitive inhibitor

To understand the catalytic mechanism of FBPA_HG the well known substrate FBP and competitive inhibitor MBP were downloaded from PubChem **[30]** and docked in identified same active site of FBPA_ HGm. In addition, to confirm the similar catalytic mechanism, the FBA and MBA also docked in proved

© 2013 Biomedical Informatics

active site of 1ZAH_Am **[18].** All docking were performed using Autodock 4.2.0 in the platform of MGLTool 1.5.4 **[31, 32].** The grid maps were generated using AutoGrid with grid box dimension 60X60X60 and 0.375 Å spacing between the grid points. Each job consisted 100 independent runs and generated log files were analyzed using MGLTool **[32].**

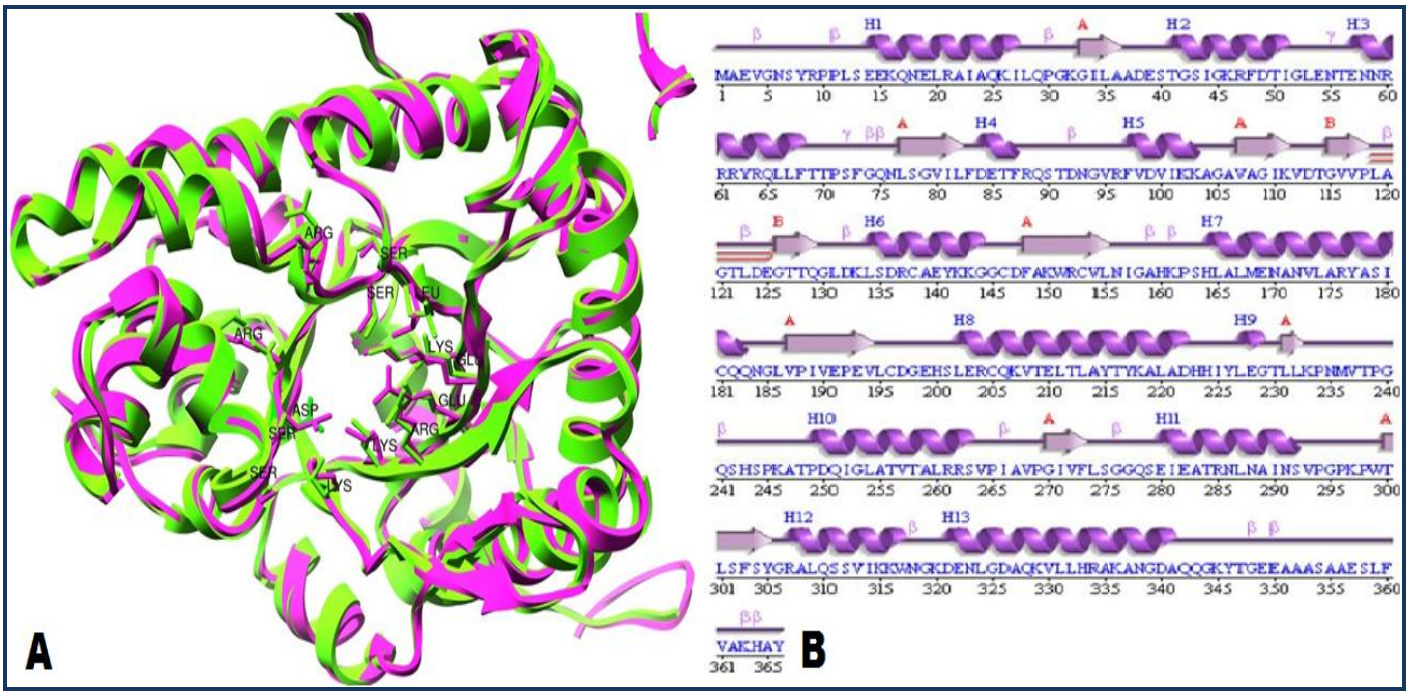

Figure 3: (A) Superimposed ribbon structure of modeled FBPA_HG (magenta) and template 1ZAH_A (green). Active site residues of FBPA_HG trapped in same active site cavity of 1ZAH shown as stick; **(B)** The secondary structural investigation for the model structure FBPA_HG.

Results:

Sequence collection and Phylogenetic analysis

The collection of available aldolase sequences of nematodes from the protein databases was an initial step towards developing a comprehensive small dataset. BLAST was used to search other amino acid sequences of aldolase in order to obtain all available sequences from the NCBI, EMBL and Swiss-port. Searching results shows all aldolase sequences from nematodes as well as nematodes keyword associated organism's aldolase sequences. Since our main focus was on aldolase sequences of nematodes, were downloaded and saved in a form of small dataset. The partial and fragmented sequences have been removed manually. The identical sequences of same nematodes *Spp*. removed from the dataset after crosschecking in EMBOSS **[13].** The screened dataset contained twenty-four unique FBPA Protein sequences given in **Table 1.** Phylogenetic analysis was performed to find out the Evolutionary relationships among dataset sequences and generated tree among each sequence shown in (**Figure 1) [15].**

The tree is classified into three major groups or cluster (namely I, II and III). The first, second and third cluster contains ten, eight and five sequences respectively. FBPA sequences of the PPNs clustered in group-II as shown in (**Figure 1)**. This group contains FBPA proteins of *Heterodera glycines* (two), *Globodera rostochiensis* (one), *Ascaris suum* (one), *Bursaphelenchus xylophilus* (one), *Caenorhabditis elegans* (two) and *Caenorhabditis brenneri* (one). Phylogenetic tree inferring FBPA sequences of PPNs having similar evolutionary relationship with group-II and slightly differ with group-I and III.

Structure models and active site identification

The structural alignment result for all FBPA sequences using DELTA-BLAST against PDB data base shown in **Table 1 [16-17].** The table contains Protein ID for best template structures for each sequence with their template searching parameter values. The chain A of FBPA Rabbit Muscle (PDB ID: 1ZAH) was the best template for twenty two protein sequences **[18].** The remaining two sequences of *Nematocida parisii* share 41% sequence identity with Chain A of Human Muscle FBPA Complex (PDB ID: 4ALD) **[33].** The Sequence of FBPA_HG having 68% identical amino acids with chain A of 1ZAH. The comparative values of validation analysis for model structures, crystal structure and simulated structures shown in **Table 2 (see supplementary material).** The stereochemical quality of each amino acid of FBPA_HG and 1ZAH_A were measured on the basis of Ramachandran plot. The PROCHECK resultant values for minimized structure of 1ZAH_Am and FBPA_HGm having better stereochemical quality in comparison to initial crystal 1ZAH_A and model FBPA_HG structure **[20, 21].** ERRAT calculates overall quality factor for non-bonded atomic interactions and higher ERRAT score means better quality of structure **[22].** The ERRAT score for minimized 1ZAH_Am and FBPA_HGm were 93.210 and 92.879 respectively, whereas the ERRAT score for 1ZAH_A and FBPA_HG were 92.744 and 30.086, respectively. The ERRAT score for FBPA_HG structure shows enhancement in atomic interaction after molecular dynamics. Evaluation of simulated structures by VERIFY3D shows better sequence-to-structure agreement in comparison to initial proteins shown in **Table 2 [23].** The overall quality G-factor score for 1ZAH_Am and FBPA_HGm were -0.30, and -0.17 respectively, indicating good quality models. A detailed

© 2013 Biomedical Informatics

secondary structural investigation of FBPA_HG with PDBsum **[24]** shows that monomer unit of structure folds into 13 Alfa-helices, 10 Strands, 19 Beta-turns and 2 Gama-turns depicted in **(Figure 3B).** The tertiary structure FBPA_HG shows close resemblance to crystal 1ZAH_A and having 0.507 Å RMSD shown in (**Figure 3A).** Low RMSD and validation statistics reflects the high structural conservation of model structure through evolution.

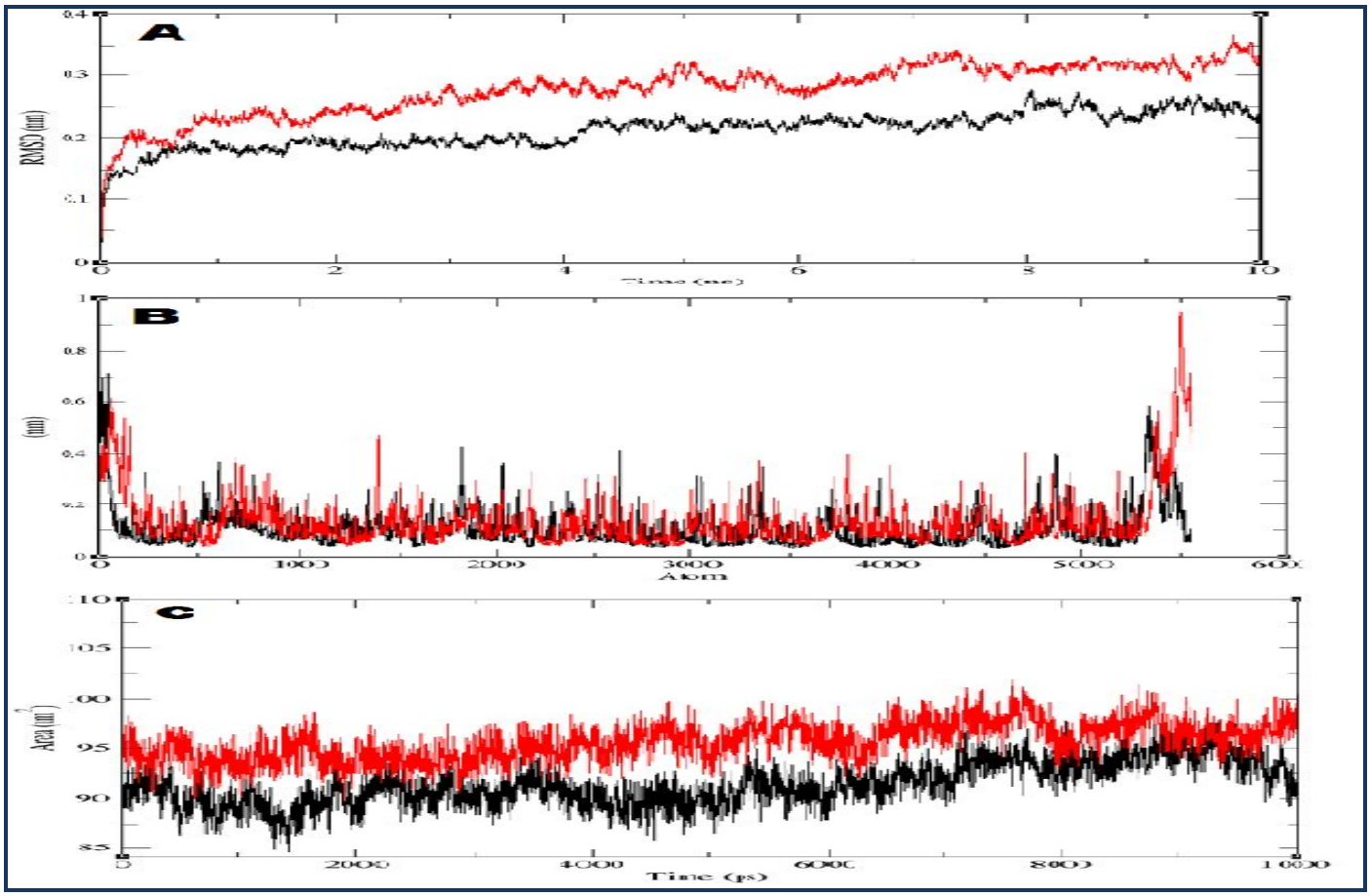

Figure 4: The comparative analysis of Root Mean Square Deviations (RMSD) plot **(A)** Root Mean Square Fluctuations (RMSF) plot; **(B)** and the total accessible surface area; **(C)** for 1ZAH_A and FBP_HG structures shown as black and red line respectively.

The tetramer structure of 1ZAH is having four chains (A, B, C and D) with identical sequences for each chain. This enzyme has defined active site residues which were playing crucial role during substrate recognition and competitive Inhibition. During enzyme-substrate recognitions a Schiff base intermediate contends and has reaction geometry with inchoate C_3–C_4 bond consistently. This intermediate reaction is catalyzed by Glu-187, which is adjacent to the Schiff base forming Lys-229. In next subsequent step the atom rearrangements take place and reaction intermediate mimics a pericyclic transition state. Then Lys-146 form Hydrogen bonding with C_4 hydroxyl that assists substrate cleavage by stabilizing the negative charge on the C4 hydroxyl. On the other hand enzyme inhibition mechanism follows the different steps. During enzyme inhibition, inhibitor form noncovalent complex which mimics a covalent carbinolamine precursor and transfer of a proton took place by the formation of hydrogen bond between inhibitor C_2 hydroxyl with Glu-187. This enables stabilization of carbinolamine transition state which reduces Schiff base formation and inhibition of active site takes place **[18].** The active site amino acid residues of FBAP_HG have been identified by Pair-Wise Multiple Sequences Alignment with template 1ZAH_A shown in **(Figure 2) [14].** The following residues of FBPA_HG are identical with crystal structure: Asp-38, Ser-40, Ser-43, Arg-47, Lys-111, Lys-150, Arg-152, Glu-191, Glu-193, Lys-233, Leu-274, Ser-275, Ser-304 & Arg-307.The superimposition of each active site residues of FBPA_HG with 1ZAH was depicted in **(Figure 3) [18].** The similar TIM barrel fold and identical active site residues of FBPA_HG may follow the similar catalytic mechanism **[12]** and it can be proved by docking of FBA and MBP ligand at active site.

Molecular dynamics simulation analysis of structures

MD simulations were performed to get stable structure of 1ZAH and FBA_HG. The main-chain root mean square deviations (RMSD) were calculated for both structures as a function of time. The resulting RMSD profiles are shown in **(Figure 4A)**. The 10ns trajectory analysis shows that both structures are behaving similar. The FBA_HG protein structure having little higher RMSD compared to the crystal 1ZAH structure. For both structures a major structural changes occurred during the initial few picoseconds leading to RMSD to ~0.25 nm, followed by smaller structural deviations for the 1ZAH and little higher for the model structure FBA_HG. The final RMSD values for 1ZAH and FBPA_HG are between ~0.25-0.35 nm. The main-chain root mean square fluctuations (RMSF),

 © 2013 Biomedical Informatics

calculated over the trajectories for 1ZAH and FBPA_HG, indicate that a large part of the residues fluctuate not more than 0.4 nm **(Figure 4B**). Both the proteins display a similar fluctuation pattern except for C terminal and N terminal regions. All catalytic site residue atoms are sharing the similar fluctuation pattern for both structure depicted in **(Figure 4B)**. However, the minimum fluctuation in substrate binding site in both proteins, leading to make a good observation of catalytic mechanism during docking studies. The solvent accessible surface area (SASA) for both structures is accessible to a solvent and it can be related to the hydrophobic core. The results indicate that the hydrophobic cores for both structures are in the range of ~85.0-95.0nm^2 and the SASA of FBPA_HG is much higher than 1ZAH_A shown in **(Figure 4C).**

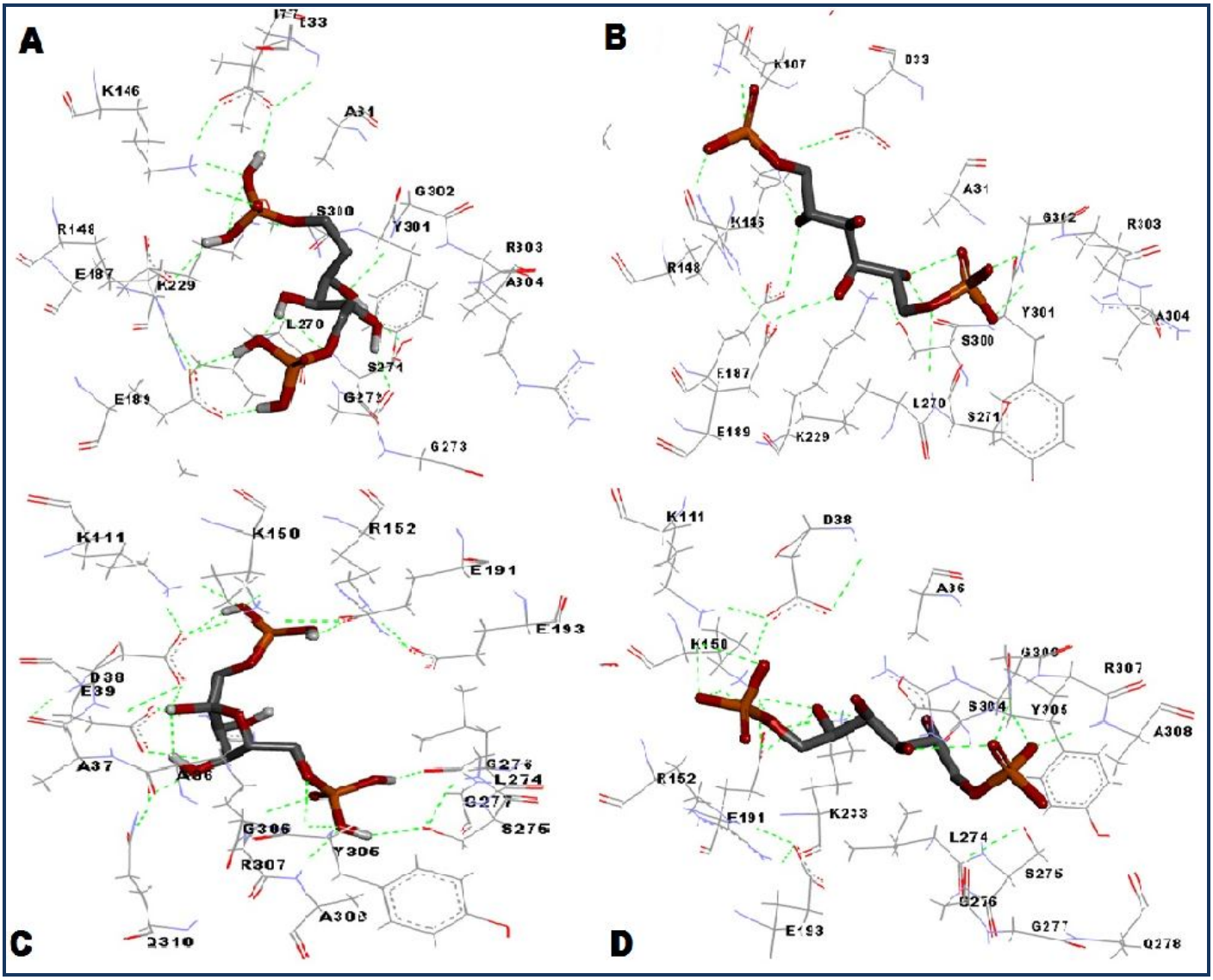

Figure 5: **(A, C)** Docked conformer of FBA shown as stick at active site of 1ZAH_Am and FBPA_HGm respectively; **(B, D)** Docked conformer of MBP shown as stick at active site of 1ZAH_Am and FBPA_HGm respectively. Each ligand forming Hydrogen bonds (green dotted line) with active site residues depicted as line.

Docking analysis

The FBPA_HG enzyme adopt the same catalytic mechanism as of class I aldolase enzyme. A covalent catalysis entailing a Schiff base formed between a lysine residues of the enzyme and ketose substrate. According to mechanism the ketose(2) of acyclic FBP substrate is attacked by reactive Lys-233 of active site of FBPA_HG in forward reaction. This reaction is catalyzed by Glu-191 and Lys-151 forming hydrogen bonds on the substrate C_4 hydroxyl and help in substrate segmentation by developing negative charges on C_4 hydroxyl during proton abstraction. Our docked results of FBP substrate in the active site of FBPA_HGm as well as 1ZAH_Am are given in **Table 3 (see supplementary material).** The best conformer of FBP at active site of 1ZAH_Am and FBPA_HG are forming nine and ten Hydrogen bonds respectively, the binding energies shows negligible difference in comparison to active site of 1ZAH_Am. In addition, the FBP are forming the similar Schiff base intermediate by forming hydrogen bonds with above said active site residues and other residues depicted in **(Figure 5A & C)**. The competitive inhibitor MBP was docked in the active site, which forms a noncovalent complex and intermediate geometry which mimics the covalent carbinolamine precursor formation. The Glu-191 forms hydrogen bonds with C_2 hydroxyl of the MBP complex and intermediate geometry which mimics the

© 2013 Biomedical Informatics

cova-lent carbinolamine precursor formation. The Glu-191 forms hydrogen-bonds with C_2 hydroxyl of the MBP inhibitor leads to the transfer of a proton from Glu-191 which catalyzes the conversion of the carbinolamine intermediate to Schiff base.

Comparative docking results of MBP inhibitor at the catalytic site of both enzymes are depicted in **Table 3**. Both docked conformer of 1ZAH_Am and FBPA_HGm shown in **(Figure 5B & D)** are forming nine Hydrogen bonds and having similar binding energy. The MBP inhibitor is forming the Hydrogen bonds with Glu-191 and Glu-187 of FBPA_HGm and 1ZAH_Am respectively. These results also support to conclude that FBPA_GR is following the similar substrate recognitions and enzyme inhibition mechanism as class I aldolase.

Conclusion:

This study was carried out to find the evolutionary and functional relationship of FBPA proteins of plant parasitic nematodes. The respective protein sequences are collected and after sequential refinement, a small dataset is built. The Phylogenetic analysis of FBPA protein sequences are clustered into three major groups according to their sequence similarity. The structural alignment of theses sequences against PDB database confirms that collected sequences belongs to class I types of aldolase. To get insight of the catalytic mechanism of *Heterodera glycines* and *Globodera rostochiensis,* molecular model were generated and validated. In subsequent step molecular dynamics simulation was performed to obtain stable structure of 1ZAH and FBPA_HG. The catalytic mechanism of FBPA_HG has been discovered on the ground by docking of substrate FBP and a competitive inhibitor MBP at the active site of both enzymes. The results confirmed that FBAP_HG and FBAP_GR are following the similar enzyme-substrate and enzyme-inhibitor reaction geometry and reaction intermediate same as class I 1ZAH aldolase. This work may be helpful to experimental biologist in controlling the parasitic infections by inhibition of aldolase.

Acknowledgement:

Authors thanks to Department of Science and Technology, New Delhi, India for supporting us financially in our ongoing project **"**Development of transgenic Wheat plant against Cereal Cyst nematode (*Heterodera Aveane*) and Sunnpest (*Eurygaster intergrices puton*) by using Bioinformatics and Genetic Engineering approaches**" Project code: INT/ILTP/A-1.28.**

References:

[1] Moravec F, *Folia Parasitologica.* 1995 **42**: 240
[2] Barrett J *et al. New York: CABI Publishing*. 1998 pp**331**–353
[3] Arnold H & Pette D, *Eur J Biochem.* 1968 **6:** 163 [PMID: 5725503]
[4] Marsh JJ & Lebherz HG, *Trends Biochem Sci.* 1991 **17:** 110 [PMID: 1412694]
[5] Lebherz HG & Rutter WJ, *Biochemistry*. 1969 **8:** 109 [PMID: 5777313]
[6] Rogers M & Keeling PJ, *J Mol Evol.* 2004 **58:** 367 [PMID: 15114416]
[7] Penhoet EE *et al. Biochemistry.* 1969 **8:** 4391 [PMID: 5353106]
[8] Penhoet EE & Rutter WJ, *J Biol Chem.* 1971 **24**6: 318 [PMID: 5542002]
[9] Plaumann M *et al. Curr Genet.* 1997 **31:** 430 [PMID: 9162115]
[10] Choi KH *et al. Biochemistry*. 2006 **45:** 8546 [PMID: 16834328]
[11] Rutter WJ & Ling KH, *Biochim Biophys Acta.* 1958 **30:** 71 [PMID: 13584398]
[12] Volker KW & Knull H, *Arch Biochem Biophys.* 1997 **338:** 237 [PMID: 9028878]
[13] Rice P *et al. Trends Genet.* 2000 **16:** 276 [PMID: 10827456]
[14] Larkin MA *et al. Bioinformatics.* 2007 **23:** 2947 [PMID: 17846036]
[15] Andrew MW *et al. Bioinformatics.* 2009 **25:** 1189 [PMCID: 2672624]
[16] http://www.rcsb.org/
[17] Grzegorz MB *et al. Biology Direct.* 2012 **7:** 12 [PMCID: 3438057]
[18] Miguel S *et al. J Biology chem.* 2005 **29**: 27262 [PMID: 15870069]
[19] Sali A & Blundell TL, *J Mol Biol*. 1993 **234**: 779 [PMID: 8254673]
[20] Laskowski RA *et al. J Biomol NMR*. 1996 **8:** 477 [PMID: 9008363]
[21] Ramachandran GN *et al. J Mol Biol*. 1963 **7:** 95 [PMID: 13990617]
[22] Colovos C & Yeates TO, *Protein Sci*. 1993 **2**: 1511 [PMID: 8401235]
[23] Eisenberg D *et al. Methods Enzymol*. 1997 **277:** 396 [PMID: 9379925]
[24] Laskowski RA *et al*. *Nucleic Acids Res.* 2005 **33:** 266
[25] Ven Der Spoel D *et al. J Comput chem.* 2005 **16:** 1701 [PMID: 16211538]
[26] Berk H *et al. J Chem Theory Comput.* 2008 **4:** 335
[27] István K *et al. J Comput Chem.* 2008 **29:** 1999 [PMID: 18366017]
[28] Berendsen HJC *et al.* Reidel Publishing Company, Dordrecht 331-342
[29] Essman U *et al. J Chem Phys*. 1995 **103:** 8577
[30] http://pubchem.ncbi.nlm.nih.gov
[31] Garrett MM *et al. J Comput Chem.* 2009 **30:** 2785 [PMCID: 2760638]
[32] http://mgltools.scripps.edu/
[33] Dalby A *et al. Protein Sci.* 1999 **8:** 291 [PMID: 10048322]

Edited by P Kangueane

Citation: **Prasad *et al.*** Bioinformation 9(1): 001-008 (2013)

License statement: This is an open-access article, which permits unrestricted use, distribution, and reproduction in any medium, for non-commercial purposes, provided the original author and source are credited

BIOINFORMATION open access

Supplementary material:

Table 1: List of final selected aldolase sequences collected from NCBI, EMBL and Uni-Port database. Phylogenetic analysis of sequences have been divided into three groups and colored according to their group I (red), group II (green) and group III (blue). The best hit template, percentage query coverage, percentage similarity, percentage identity and their respective values for each sequence obtained after structural alignment against PDB database.

S. No.	Accession Number	Types of Aldolase	Nematodes family	Best Hit Template	% Query Coverage	% Similarity	% Identity
1	G0NGQ0	Fructose-bisphosphate aldolase	*Caenorhabditis brenneri*	1ZAH_A	98	77	67
2	E5SNV8	Fructose-bisphosphate aldolase	*Trichinella spiralis*	1ZAH_A	98	77	67
3	ADT61995	Aldolase	*Haemonchus contortus*	1ZAH_A	98	80	68
4	BAA12092	Fructose-bisphosphate aldolase	*Caenorhabditis elegans*	1ZAH_A	97	75	65
5	EDP37892	Fructose-bisphosphate aldolase	*Brugia malayi*	1ZAH_A	86	66	53
6	ADY45376	Fructose-bisphosphate aldolase	*Ascaris suum*	1ZAH_A	95	80	70
7	AFL46381	Fructose bisphosphate aldolase	*Dirofilaria immitis*	1ZAH_A	98	80	69
8	AAD38403	Fructose-bisphosphate aldolase	*Onchocerca volvulus*	1ZAH_A	98	80	69
9	EJD76644	fructose-bisphosphate aldolase	*Loa loa*	1ZAH_A	86	81	70
10	EFO24470	Fructose-bisphosphate aldolase	*Loa loa*	1ZAH_A	98	80	69
11	G0PE81	Fructose-bisphosphate aldolase	*Caenorhabditis brenneri*	1ZAH_A	97	76	65
12	AAR09171	Fructose-bisphosphate aldolase	*Heterodera glycines*	1ZAH_A	97	75	66
13	AAG47838	Fructose-bisphosphate aldolase	*Heterodera glycines*	1ZAH_A	97	75	66
14	AAN78210	Fructose-bisphosphate aldolase	*Globodera_rostochiensis*	1ZAH_A	97	75	67
15	BAA12091	Fructose-bisphosphate aldolase 1	*Caenorhabditis elegans*	1ZAH_A	98	77	66
16	F1L6S0	Fructose-bisphosphate aldolase	*Ascaris suum*	1ZAH_A	85	75	64
17	G8JY45	Fructose-bisphosphate aldolase	*Caenorhabditis elegans*	1ZAH_A	94	75	65
18	D1MBS1	Fructose-bisphosphate aldolase	*Bursaphelenchus xylophilus*	1ZAH_A	90	75	65
19	H8ZCZ6	Fructose-bisphosphate aldolase class-I	*Nematocida Sp.*	1ZAH_A	95	60	43
20	EDP36623	Fructose-bisphosphate aldolase	*Brugia malayi*	1ZAH_A	98	81	69
21	EDP36623	Fructose-bisphosphate aldolase	*Brugia malayi*	1ZAH_A	98	81	69
22	I3EDM9	Fructose-bisphosphate aldolase class-I	*Nematocida parisii*	4ALD_A	97	59	41
23	I3EQ13	Fructose-bisphosphate aldolase class-I	*Nematocida parisii*	4ALD_A	97	59	41
24	F1KQJ9	Fructose-bisphosphate aldolase 1	*Ascaris suum*	1ZAH_A	95	73	53

Table 2: Structure validation scores generated by various validation algorithms, for initial chain A of 1ZAH and model of FBPA_HG as well as for their Energy minimized structure 1ZAH_A and FBPA_HGm

Ramachandran Plot statistics	1ZAH_A	1ZAH_Am	FBPA_HG	FBPA_HGm
% Amino acid in most favored regions	88.5%	90.1%	69.4%	88.2%
% Amino acid in additional allowed regions	10.9%	9.3%	25.5%	9.9%
% Amino acids in generously allowed regions	0.6%	0.6%	4.8%	1.9%
% Amino acids in disallowed regions	0.0%	0.0%	0.3%	0.0%
Errat score	92.744	93.210	30.086	92.879
Verify_3D score	90.03	93.13	87.47	92.74
Overall G-factor score	0.36	-0.30	-1.12	-0.17

Table 3: Comparative docking results of best conformer for FBP and MBP in the catalytic site of 1ZAH_Am and FBPA_HGm

Target protein	Fructose-1, 6-bisphosphate (FBP)			Mannitol-1, 6 bisphosphate (MBP)		
	Binding Energy KJ/mol	No. of Hydrogen Bonds	H-Bonding Residues	Binding Energy KJ/mol	No. of Hydrogen Bonds	H-Bonding Residues
1ZAH_Am	-6.24	9	Asp-33, Lys-107, Lys-146, Glu-187,Glu-189, Lys-229, Gly-272, Ser-300, Gly-202 Arg-303	-6.80	9	Lys-107, Lys-146, Arg-148, Glu-187, Lys-229, Ser-300, Gly-202 Arg-303
FBPA_HGm	-6.16	10	Asp-38, Lys-111, Lys-150, Glu-191, Ser-275, Gly-276, Gly306, Arg-307, Ala-308, Gln-310	-6.80	9	Lys-111, Lys-150, Glu-191, Ser-275, Gly-276, Gly306, Arg-307, Ala-308

© 2013 Biomedical Informatics